Check for updates

Stroke

BASIC AND TRANSLATIONAL SCIENCES

Design of a Stem Cell–Based Therapy for Ependymal Repair in Hydrocephalus Associated With Germinal Matrix Hemorrhages

Luis M. Rodriguez-Perez, PhD*; Betsaida Ojeda-Pérez, MS*; Javier López-de-San-Sebastián, BSc; María García-Bonilla, PhD; Marcos González-García, BSc; Beatriz Fernández-Muñoz, PhD; Rosario Sánchez-Pernaute, MD, PhD; María L. García-Martín, PhD; Dolores Domínguez-Pinos, MD, PhD; Casimiro Cárdenas-García, PhD; Antonio J. Jiménez, PhD†; Patricia Paez-Gonzalez, PhD†

BACKGROUND: In preterm birth germinal matrix hemorrhages (GMHs) and the consequent posthemorrhagic hydrocephalus (PHH), the neuroepithelium/ependyma development is disrupted. This work is aimed to explore the possibilities of ependymal repair in GMH/PHH using a combination of neural stem cells, ependymal progenitors (EpPs), and mesenchymal stem cells.

METHODS: GMH/PHH was induced in 4-day-old mice using collagenase, blood, or blood serum injections. PHH severity was characterized 2 weeks later using magnetic resonance, immunofluorescence, and protein expression quantification with mass spectrometry. Ependymal restoration and wall regeneration after stem cell treatments were tested in vivo and in an ex vivo experimental approach using ventricular walls from mice developing moderate and severe GMH/PHH. The effect of the GMH environment on EpP differentiation was tested in vitro. Two-tailed Student *t* or Wilcoxon-Mann-Whitney *U* test was used to find differences between the treated and nontreated groups. ANOVA and Kruskal-Wallis tests were used to compare >2 groups with post hoc Tukey and Dunn multiple comparison tests, respectively.

RESULTS: PHH severity was correlated with the extension of GMH and ependymal disruption (means, 88.22% severe versus 19.4% moderate). GMH/PHH hindered the survival rates of the transplanted neural stem cells/EpPs. New multiciliated ependymal cells could be generated from transplanted neural stem cells and more efficiently from EpPs (15% mean increase). Blood and TNFα (tumor necrosis factor alpha) negatively affected ciliogenesis in cells committed to ependyma differentiation (expressing Foxj1 [forkhead box J1] transcription factor). Pretreatment with mesenchymal stem cells improved the survival rates of EpPs and ependymal differentiation while reducing the edematous (means, 18% to 0.5% decrease in severe edema) and inflammatory conditions in the explants. The effectiveness of this therapeutical strategy was corroborated in vivo (means, 29% to 0% in severe edema).

CONCLUSIONS: In GMH/PHH, the ependyma can be restored and edema decreased from either neural stem cell or EpP transplantation in vitro and in vivo. Mesenchymal stem cell pretreatment improved the success of the ependymal restoration.

GRAPHIC ABSTRACT: A graphic abstract is available for this article.

Key Words: edema ■ ependyma ■ hydrocephalus ■ mesenchymal stem cells ■ neural stem cells

Downloaded from http://ahajournals.org by on February 4, 2025

Correspondence to: Patricia Paez-Gonzalez, PhD, Departamento de Biología Celular, Genética y Fisiología, Facultad de Ciencias, Universidad de Málaga, Campus de Teatinos, 29071 Malaga, Spain, Email patricia.paez.gonzalez@uma.es; or Antonio J. Jiménez, PhD, Departamento de Biología Celular, Genética y Fisiología, Facultad de Ciencias, Universidad de Málaga, Campus de Teatinos, 29071 Malaga, Spain, Email ajjimenez@uma.es
*L.M. Rodriguez-Perez and B. Ojeda-Pérez contributed equally.
†A.J. Jiménez and P. Paez-Gonzalez contributed equally.
Supplemental Material is available at https://www.ahajournals.org/doi/suppl/10.1161/STROKEAHA.123.044677.
Preprint posted on BioRxiv April 13, 2023. doi: https://doi.org/10.1101/2023.04.13.536749.
For Sources of Funding and Disclosures, see page 1073.
© 2024 The Authors. *Stroke* is published on behalf of the American Heart Association, Inc., by Wolters Kluwer Health, Inc. This is an open access article under the terms of the Creative Commons Attribution Non-Commercial-NoDerivs License, which permits use, distribution, and reproduction in any medium, provided that the original work is properly cited, the use is noncommercial, and no modifications or adaptations are made.
Stroke is available at www.ahajournals.org/journal/str

Nonstandard Abbreviations and Acronyms

DAPI	4′,6-diamidino-2-phenylindole
EpP	ependymal progenitor
GMH	germinal matrix hemorrhage
IVH	intraventricular hemorrhage
LV	lateral ventricle
modGMH/PHH	moderate germinal matrix hemorrhage/posthemorrhagic hydrocephalus
modPHH	moderate posthemorrhagic hydrocephalus
MSC	mesenchymal stem cell
NSC	neural stem cell
PHH	posthemorrhagic hydrocephalus
sevGMH/PHH	severe germinal matrix hemorrhage/posthemorrhagic hydrocephalus
sevPHH	severe posthemorrhagic hydrocephalus
TNFα	tumor necrosis factor alpha

Germinal matrix hemorrhages (GMHs), intraventricular hemorrhages (IVHs), and subsequent posthemorrhagic hydrocephalus (PHH) are major causes of morbidity and mortality in the premature neonatal population and require lifelong, complex neurosurgical care.[1,2] PHH injuries include periventricular edema and neuroinflammation.[3]

Disruption of multiciliated ependyma development[4,5] is a relevant and key event associated with GMH/IVH/PHH. The ependyma constitutes a cell barrier between the brain parenchyma and the ventricle cerebrospinal fluid.[6,7] Lysophosphatidic acid, iron, and other blood components can be involved in ependymal disruption and dysfunction.[8–10] Thus, ependyma can be considered a key therapeutic target because of its relevance for hydrocephalus occurrence and role in cerebrospinal fluid circulation and physiology.[11]

There is no therapy to treat all the consequences associated with PHH. Therapies with neural stem cells (NSCs)[12,13] and mesenchymal stem cells (MSCs)[14–16] have reported promising results in hydrocephalus of obstructive and posthemorrhagic origins. However, in no case did the ependyma regenerate.[14,16,17]

This study investigates the possibility of directly repairing the ependyma in PHH using NSCs and ependymal progenitor (EpP) cells and the effect of an MSC environment. For this purpose, PHH has been induced in neonatal mice at a developmental stage equivalent to that when neurological processes are affected in human cases after GMH/IVH.[18] Intracerebroventricular injection of blood and blood serum was used to induce PHH. In addition, GMH was induced by collagenase injection, which has been proven to mimic human PHH.[2,19] The possibility and efficiency of ependymal restoration were tested in a new ex vivo approach using ventricular wall explants of the mice generated with moderate GMH/PHH (modGMH/PHH) and severe GMH/PHH (sevGMH/PHH). The effect of inflammatory microenvironment modification by bone marrow–derived MSCs was investigated. Ependyma restoration and tissue improvement were corroborated in in vivo experiments.

METHODS

The data sets used and analyzed during the current study are available from the corresponding authors upon reasonable request. A detailed Methods section is available in the Supplemental Material.

Experimental Animals

The design of the experiments and animal housing, handling, care, and processing were conducted following the European and Spanish laws (RD53/2013 and 2010/63UE) and the ARRIVE guidelines (Animal Research: Reporting of In Vivo Experiments). According to the current legislation, experimental procedures (protocol 23/04/2019/069) were approved by the Institutional Animal Care and Use Committee of the University of Malaga (Spain) and the Regional Government Council (Junta de Andalucía, Spain).

Mice (C57/BL-6J strain) were obtained from Charles River Laboratory and bred in the Animal Experimentation Service of the University of Malaga at 22 °C with a 12:12 light/dark cycle and standard food and water available ad libitum. Mice of both sexes were used in all the experiments.

GVH/PHH Induction

Four-day-old mice were anesthetized with 2% isoflurane in 0.5 L/min oxygen anesthesia and injected with blood serum in the right lateral ventricle (LV) or both right and left LVs, whole blood, or collagenase I in the subventricular germinal matrix of each hemisphere, to produce GMH/IVH conditions. Mice were euthanized at different time points after the GMH/IVH induction and used to validate the model, and in ex vivo and in vivo transplantation experiments.

Immunofluorescence in Brain Sections

Eighteen-day-old mice (14 days after GVH/PHH induction) from the different experimental groups were analyzed: blood serum in the right LV, n=7; blood serum in both LVs, n=4; whole blood, n=7; collagenase, n=9; controls without any injection, n=9; controls with saline serum injection, n=6. Frozen sections were obtained and processed for immunofluorescence. Nuclei staining was performed with DAPI (4′,6-diamidino-2-phenylindole).

Magnetic Resonance Imaging

Magnetic resonance imaging experiments were on a 9.4T Bruker Biospec small animal magnetic resonance imaging system (Bruker Biospec; Bruker BioSpin, Ettlingen, Germany) equipped

Downloaded from http://ahajournals.org by on February 4, 2025

with a 40-mm quadrature bird-cage resonator and 440-mT/m gradients. Normal mice (n=6) and mice exhibiting moderate PHH (modPHH; n=4) and severe PHH (sevPHH; n=3) were anesthetized and monitored throughout the experiment. The acquisition protocol consisted of a high-resolution T2-weighted rapid acquisition with relaxation enhancement sequence with fat suppression and 3-dimensional fast imaging with steady precession.

Ultra-High-Performance Liquid Chromatography–High-Resolution Mass Spectrometry Analysis of Protein Expression

For ultra-high-performance liquid chromatography–high-resolution mass spectrometry, the caudal cerebral wall was dissected from control mice (n=10), mice with modPHH (n=7), and mice with sevPHH (n=6) at 18 days of age, immediately after euthanization by cervical dislocation. Proteins from the samples were purified, and abundance ratios were directly calculated from the grouped protein abundances. ANOVA was based on the abundance of individual proteins or peptides.

Ventricle Wall Explant In Vitro Assays

Forty-eight hours after GMH/PHH induction with collagenase or blood serum, mice were euthanized by decapitation; the brain was dissected and classified according to GMH extension and LV size into modGMH/PHH or sevGMH/PHH. Explants from the lateral wall of the LV, the striatal wall, were carefully positioned on Millicell culture inserts into 6-well culture plates (3 explants per insert; Figure S1) containing 1 mL of sterile organotypic culture medium.

The explants used to study the survival of transplanted stem cells and their progenies were fixed and immunostained or tested with Evans blue.

Bone Marrow–Derived MSC Isolation and Culture

Bone marrow–derived MSCs were obtained and characterized as described previously.[15] Detached cells were resuspended in saline serum to pretreat explants, primary cultures, or animals in vivo.

NSC Isolation and Culture

The subventricular zone of the rostral-dorsal striatal wall in newborn male and female mice was dissected and mechanically dissociated to obtain NSCs.

EpP Cell Collection

EpPs were obtained from newborn mice. In this case, the subventricular zone of the medial striatal ventricle wall was dissected out and mechanically dissociated. Cells were plated at 500 000 cells/mL using the same media on poly D-lysine–coated round coverslips. Then, the EpPs were differently processed to treat explants, animals in vivo, or to study in primary cultures.

Stem Cell Transplantation in Ventricular Wall Explants

Before application, NSCs, EpPs, and MSCs were labeled in vitro by adding fluorescent cell tracker dyes (Figure S2). The stem cells were resuspended in their vehicle solution (NSCs and EpPs, 10 000 cells/µL; MSCs, 10 000 cells/µL). A volume of 1 µL was used per ventricular wall. Controls were performed by injection of vehicle solution. Experiments were performed with 3 explants per experimental condition and replicated 5×, a total of 15 explants per experimental condition.

In Vitro Differentiation of EpP Cells Under the Effect of Blood Components

EpPs were plated at 500 000 cells/mL on poly D-lysine–coated coverslips (5 coverslips per well) and cultured in N5 medium. Twenty-four hours after starting differentiation with N5, blood and blood serum were applied to the culture (50 µL per 500 000 cells/mL). In the case of TNFα (tumor necrosis factor alpha), it was applied every 2 days at 50 ng/mL for a maximum of 9 days. The cells were fixed and immunostained in the different treatments at 3, 6, and 9 days to detect Foxj1 (forkhead box J1 transcription factor) protein and cilia. Each condition was replicated 5×.

In Vitro Differentiation Recovery of EpP Cells in the Presence of Blood Components and Bone Marrow–Derived MSCs

MSCs (20 000 cells/mL) were added once to the EpP primary culture, 24 hours after the medium was switched to N5, and maintained with the different treatments for 9 days. Blood, blood serum, and the inflammatory cytokine TNFα were also applied as described above. Each condition was replicated 7×.

Evans Blue Assay to Test the Brain Parenchymal Effect

LV wall explants from mice with collagenase-induced moderate GMH were positioned on Millicell culture inserts in 6-well culture plates (3 explants per insert). After 6 hours in vitro, explants were transplanted with MSCs. EpPs were transplanted 24 hours later. The medium was partially changed every 48 hours. Evans blue was applied after 7 days of treatment, and the tissue was fixed. The staining intensity indicated the grade of tissue damage and edematous status. For each experimental condition, we used 6 explants.

Cytokine Content in Culture Media From Treated Explants

Media were collected to detect cytokines after different treatments: without explants as the baseline for the cytokine kit array (empty wells), nontreated explants (9 explants), MSC-pretreated explants (9 explants), and sequential transplantation of MSCs and EpPs in explants (9 explants). A kit array was used to detect the expression of 62 cytokines. To obtain an accurate cytokine value for nontreated and treated explants, we subtracted the baseline expression of cytokines in the media with no explants for every case.

In Vivo Transplantation of MSCs and EpPs

Two experiments were performed 4 days after GMH/PHH induction with collagenase. In the first, MSCs were transplanted

Downloaded from http://ahajournals.org by on February 4, 2025

 Stroke. 2024;55:1062–1074. DOI: 10.1161/STROKEAHA.123.044677

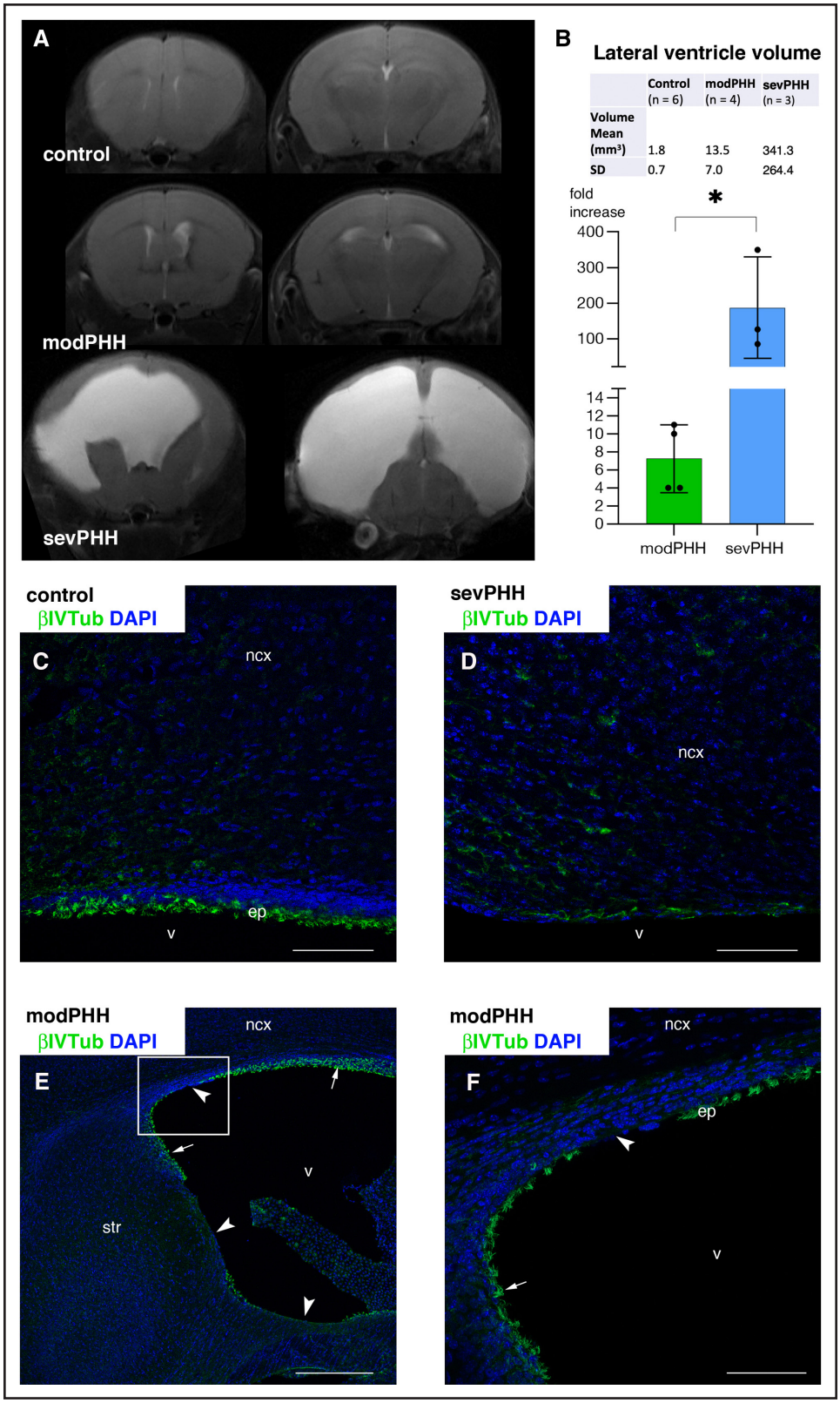

Figure 1. Differential lateral ventricle enlargement after germinal matrix hemorrhage induction by collagenase injection. Mice exhibited mild ventriculomegaly (moderate posthemorrhagic hydrocephalus [modPHH]) and large ventriculomegaly (severe posthemorrhagic hydrocephalus [sevPHH]) compared with a normal mouse (control). **A**, T2 magnetic resonance images. **B**, **Top**, Representative examples of lateral ventricle volume in the different experimental groups. **B**, **Bottom**, Representation of the volume fold increase compared with the normal mice mean. *Student *t*, *$P<0.05$, mean±SD (control, n=6; modPHH, n=4; sevPHH, n=3), *$P<0.05$, **$P<0.01$, ANOVA/Tukey. **C** through **F**, Ependymal denudation (arrowheads) in the lateral ventricle detected by cilia immunostaining with βIVTub (βIV-tubulin; arrows). Cell nuclei are stained with DAPI (4′,6-diamidino-2-phenylindole; blue). Scale bars, 77 µm (**C**, **D**, and **F**) and 300 µm (**E**). ep indicates ependyma; ncx, neocortex; str, striatum; and v, ventricle lumen.

Downloaded from http://ahajournals.org by on February 4, 2025

with 10 000 EpPs/µL or the vehicle (control). In the second, GMH/PHH-induced animals were injected with 10 000 MSCs/µL (or vehicle in control) and 2 days later with 10 000 EpPs/µL (or vehicle in control). In both experiments, 12 days later, mice were processed as described in GVH/PHH induction section. Ventricular walls were dissected and classified as described in stem cell transplantation in ventricular wall explants section. Evans blue was applied to detect edematous areas. Ventricle walls of 5 animals per experimental condition were analyzed.

Image Analysis and Quantification

Confocal and fluorescence images were obtained in batches with control and experimental samples imaged under identical instrument settings. Quantification was manually and blindly performed.

Statistics

Samples were analyzed using GraphPad 9.2.0 (GraphPad Software, San Diego, CA) and Microsoft Excel 16.71. To achieve 80% power with a 5% significance level, the required sample size was estimated using mean differences and pooled SDs from preliminary quantifications. Normality was assessed with the Shapiro-Wilk test. For Student *t* test or the Wilcoxon-Mann-Whitney *U* test, 2-tailed test was used. ANOVA and Kruskal-Wallis tests were used to compare >2 groups with post hoc Tukey and Dunn multiple comparison tests, respectively. $P<0.05$ was considered statistically significant.

RESULTS

Generation of Moderate and sPHH

PHH was induced by injection with whole blood into the right LV, blood serum (right LV or both LVs), and collagenase into the germinal matrix in both hemispheres. Neuropathological analysis showed that 2 groups of animals were identified. The first group exhibited sevPHH with at least a 50-fold increase in the LV volume. It was obtained with blood serum injection (2.75% of 11 total mice by injection in right LV and 7.69% of 11 total mice by injections in both LVs), whole blood (18.2% of 13 total mice), or collagenase (55.5% of 33 total mice). Five mice died

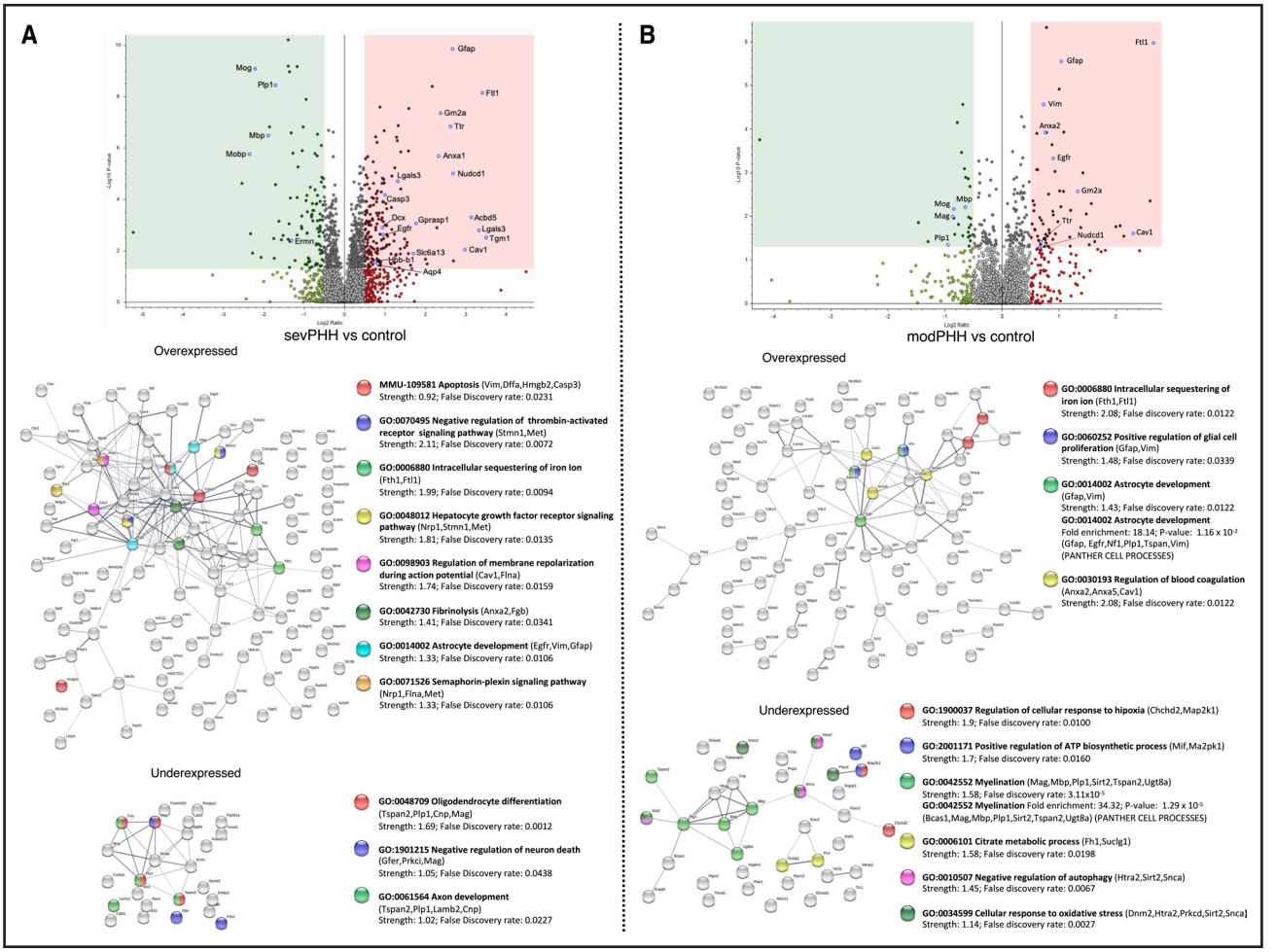

Figure 2. Analysis of differential protein expression is posthemorrhagic hydrocephalus.
Overexpressed and underexpressed proteins comparing (**A**) mice with severe posthemorrhagic hydrocephalus (sevPHH; n=6) and (**B**) moderate posthemorrhagic hydrocephalus (modPHH; n=7) with normal mice (control, n=10). Volcano plots (**top**), protein-protein interaction networks, and functional enrichment analysis (**bottom**) are represented. For details, see the Supplemental Material and Tables S1 through S14.

Downloaded from http://ahajournals.org by on February 4, 2025

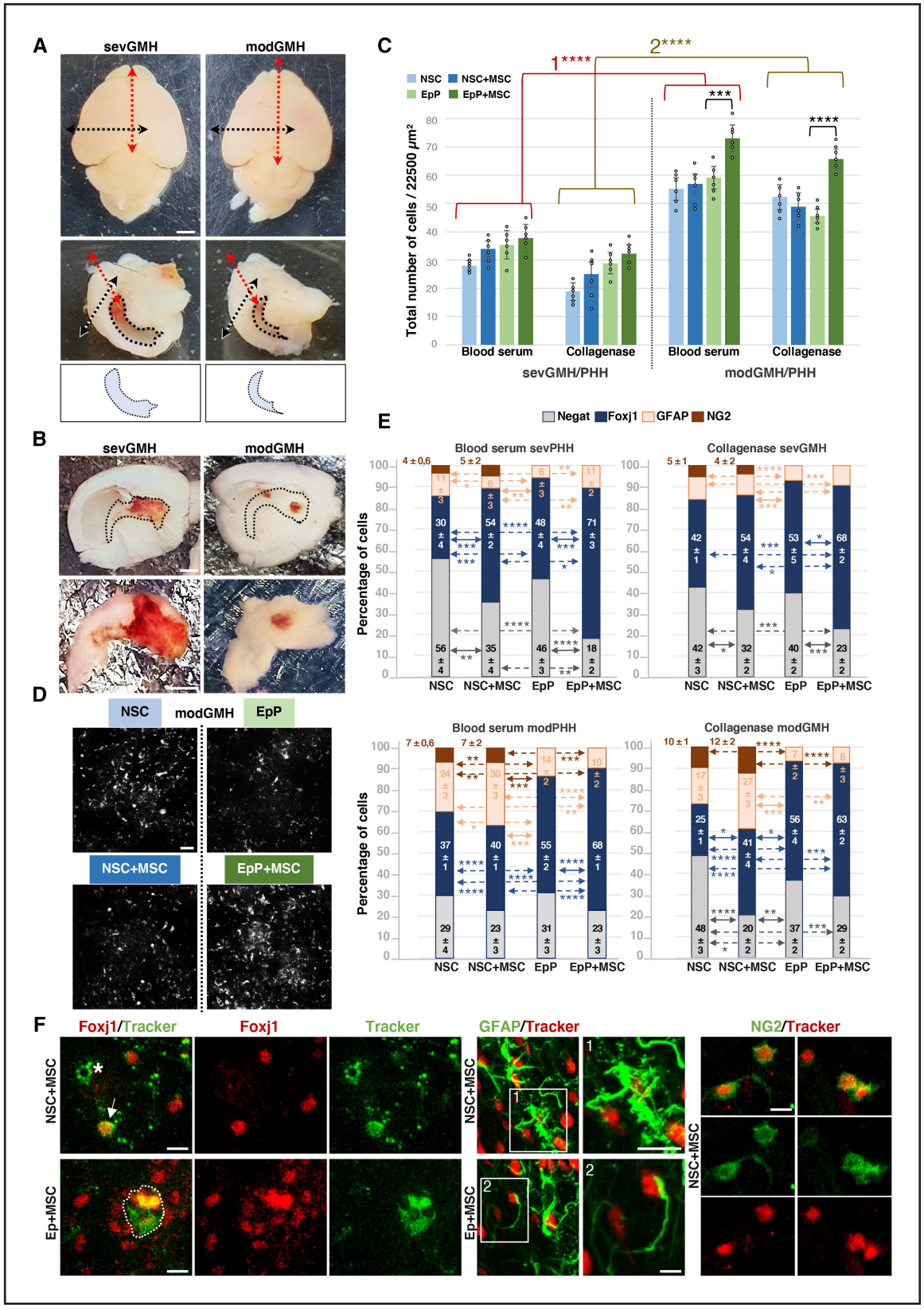

Figure 3. Survival and differentiation of ependymal progenitors (EpPs) and neural stem cells (NSCs) in explants.
A, Dissection of explants. The double-ended red and black dashed lines represent the incision planes that expose cerebral-ventricular cavities. **Top**, Isolated brain previous dissection. **Bottom**, Differential ventricular dilatation (dotted lines). **B**, Exposed lateral ventricular striatal walls (dotted lines) showing the periventricular hemorrhages (**top**) and dissected explants (**bottom**). **Left**, Mouse with severe germinal matrix hemorrhage (sevGMH) showing extensive hemorrhage. **Right**, Mouse with moderate germinal matrix hemorrhage (modGMH). **C**, Total number of (*Continued*)

Downloaded from http://ahajournals.org by on February 4, 2025

a day after the injection (not classified, Figure 1A and 1B). Another significant percentage of mice developed LV mild ventriculomegaly, with at least a 2-fold volume increase compared with normal mice after injection with blood serum into the right LV (54.5%) or in both ventricles (61.5%), whole blood (27.3%), and collagenase (30.3%; Figure 1A and 1B). The latter mice were considered to have an modPHH, as confirmed by histopathologic and protein expression analyses described below.

Mice With Moderate and Severe Forms of PHH Shared Common Neuropathological Events

The same neuropathological events were detected with the different procedures to produce PHH (Figures S3 through S5). However, this model was selected for testing the therapies based on the higher efficiency of collagenase injections to produce GMH/PHH and how it mimics human disease.[19] The neuropathology of this model was then thoroughly analyzed.

Mice with modPHH and sevPHH (Figure 1C through 1F; Figure S3) showed different extensions of LV surfaces denuded of ependyma (sevPHH, n=5; mean, 88.22% [SD, ±10.09]; modPHH, n=4; mean, 19.04% of the LV surface [SD, ±8.34]; $P<0.0001$, t=11, df=7, unpaired 2-tailed Student *t* test). In addition, mice with both sevPHH and modPHH presented a periventricular white matter microglia and astroglia reaction mostly associated with ependyma-denuded surfaces (Figures S6 and S7).

The analysis of overexpressed proteins revealed, in both sevPHH and modPHH, alterations in molecular pathways indicative of IVH consequences (Figure 2; Figures S7 and S8; Tables S1 through S6). These results corroborated the existence of 2 groups of animals, sevPHH mice and modPHH mice, where stem cell therapy could have differential effects according to ependyma disruption and inflammatory conditions.

Developing an Ex Vivo System to Test Ependymal Restoration

To try ependymal restoration, we tested the combinatory sets of selected stem cell types: NSCs or EpPs as a source of new ependyma and MSCs to improve the hosting environment. For this purpose, it was necessary to evaluate the efficiency of the transplantation, integration, and differentiation of the selected stem cells.

Based on our previous results,[20] MSCs would need to be transplanted shortly after GMH/IVH induction. However, a few days after the induction of GMH/IVH, it was impossible to identify the GMH extension or whether the animals were developing modPHH or sevPHH by analyzing external physical signs or the behavior of the animal. The cerebrospinal fluid content highly varies between the modPHH and sevPHH mice; therefore, the unknown initial concentration of the transplanted cells would make it impossible to determine the efficiency of the treatments. A new ex vivo experimental system was developed using ventricular wall explants from GMH/IVH-induced animals to overcome the problem. Collagenase injection was chosen because it showed high efficiency and consistency and mimicked blood injection. Blood serum condition was kept for testing blood factors independently of the cellular components.

Three days after IVH/GMH induction, animals were euthanized and ventricular walls exposed and classified into developing modGMH/PHH or sevGMH/PHH according to the GMH extension, ventricular size, and periventricular damage (Figure 3A and 3B). Then, walls were dissected, and explants were generated and cultured as an ex vivo system where the different combinations of stem cell therapies could be tested (Figure S1). In this controlled system, the initial concentration of transplanted stem cells, stem cell integration, and differentiation into ependyma could be followed and studied.

Survival Rates of Transplanted Stem Cells According to the Severity of PHH Development

The survival rate of NSCs and EpPs (including their progeny) was studied 7 days after transplantation. The survival rate of the transplanted NSCs and EpPs was higher in the explants from modGMH/PHH mice than from sevGMH/PHH mice (Figure 3C; Table S7). Pretreatment with MSCs improved the survival rate of EpPs but not NSCs in explants from modGMH/PHH mice but had no effect on explants from sevGMH/PHH mice (Figure 3C and 3D; Table S7).

Differentiation of EpP Cells and NSCs Into Ependymal Cells

The efficiency of EpPs and NSCs in producing cells committed to be ependyma expressing the transcription

Figure 3 Continued. cells that survived 7 d after transplantation. Mean±SD (bars), n=6 in each condition, ***$P<0.001$, ****$P<0.0001$, ANOVA/Tukey. Differences in the survival rates were significant between mice with moderate germinal matrix hemorrhage/posthemorrhagic hydrocephalus (modGMH/PHH) and severe germinal matrix hemorrhage/posthemorrhagic hydrocephalus (sevGMH/PHH) with and without mesenchymal stem cell (MSC) pretreatment (1 and 2). **D**, Transplanted cells, labeled with a tracker, on the surface of the explant. **E**, Differentiation of the transplanted NSCs and EpPs into Foxj1+ (forkhead box J1 transcription factor) cells, GFAP+ (glial fibrillary acidic protein) cells, and NG2+ (neural/glial antigen 2) cells 7 d after transplantation. Transplanted negative cells are also shown. Mean±SD, n=5 in each condition. *$P<0.05$, **$P<0.01$, ***$P<0.001$, ****$P<0.0001$, ANOVA/Tukey. **F**, Sample pictures used for quantification in **D** from animals with modGMH induced by collagenase. **Left**, NSCs and EpPs (green tracker, arrow) expressing Foxj1. Asterisk points to an NSC lacking expression of Foxj1. A cluster of Foxj1+ cells derived from EpPs is framed. **Middle**, NSCs and EpPs (red tracker) expressing GFAP. Details (1 and 2) are shown on the **right**. Scale bars: 2 mm (**A** and **B**), 30 µm (**D**), and 20 µm (**F**).

Downloaded from http://ahajournals.org by on February 4, 2025

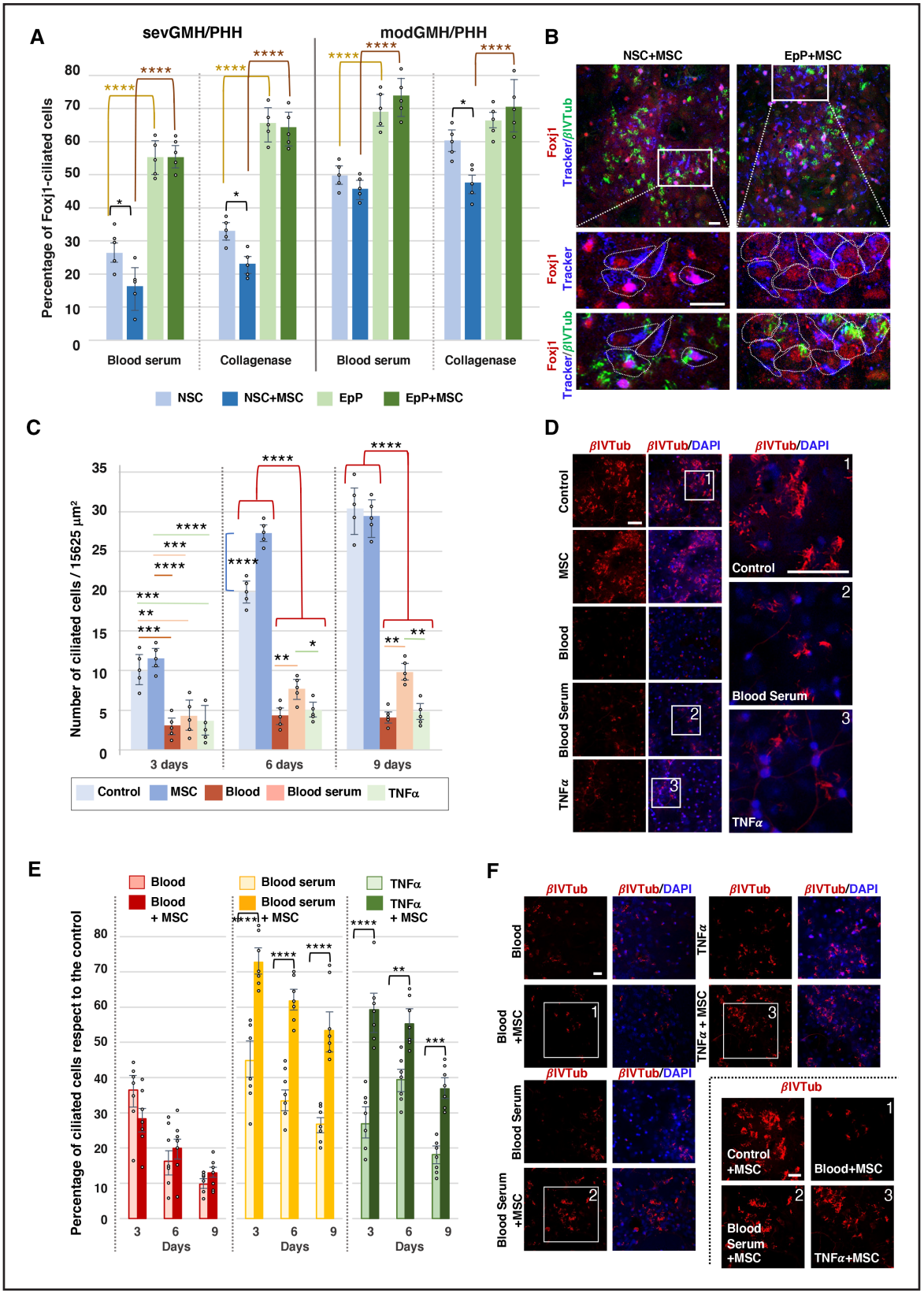

Figure 4. Differentiation into multiciliated ependyma of Foxj1+ (forkhead box J1 transcription factor) cells.
A, Percentages of ciliated Foxj1+ cells after 7 d. Mean±SD (bars), n=5, **P*<0.05, *****P*<0.0001, ANOVA/Tukey. **B**, Multiciliated progeny after 7 d in ventricular wall explants from the animals with moderate germinal matrix hemorrhage (modGMH) generated by collagenase injection. Neural stem cell (NSC)–derived and ependymal progenitor (EpP)–derived cells are labeled with a cell tracker. **Bottom**, Details framed at the **top**. Some Foxj1+ cells are multiciliated (βIVTub [βIV-tubulin]), indicating that they fully differentiate into ependymal cells. **C**, Rates from EpPs (*Continued*)

Downloaded from http://ahajournals.org by on February 4, 2025

factor Foxj1 was investigated (Figure 3E). For description purposes, positive cells derived from EpPs and NSCs are called ^{EpP}Foxj1+ and ^{NSC}Foxj1+, respectively. In the LV wall explants, the ^{EpP}Foxj1+ percentage was higher than the ^{NSC}Foxj1+ percentage (Figure 3E; Table S8). This result was consistent for blood serum and collagenase injections (Figure 3E; Table S8). Therefore, and not unexpectedly, EpPs generated more Foxj1+ cells than NSCs. Notably, the MSC pretreatment in explants increased the rates of ^{EpP}Foxj1+ and ^{NSC}Foxj1+ cells (Figure 3E and 3F; Table S8).

In addition to Foxj1+ cells derived from NSCs or EpPs, other main cell types derived from transplanted stem cells were analyzed. The presence of NG2+ (neural/glial antigen 2) and GFAP+ (glial fibrillary acidic protein) cells and transplanted cells that did not express any of these markers (Foxj1−/NG2−/GFAP−), thus called negative cells, was quantified. In the case of transplanted NSCs, other cells expressing NG2 and GFAP were generated (Figure 3E and 3F; Table S8). The transplanted EpPs generated GFAP+ cells but not NG2+ cells under all studied conditions (Figure 3E and 3F; Table S8). Pretreatment with MSCs did not change the type of progeny generated from NSCs or EpPs for GFAP and NG2 (Figure 3E; Table S8). However, for NSC and EpP transplantation, MSC pretreatment revealed a generalized decrease in negative cells (Foxj1−/NG2−/GFAP−) that agreed with the increased rate of Foxj1 positive-derived cells (Figure 3E; Table S8).

Cilia Development From Cells Committed to Ependymal Differentiation Under PHH Conditions

The efficiency of Foxj1+ cells in terminally differentiating into multiciliated ependymal cells was investigated. A percentage of Foxj1+ cells did not develop multicilia; therefore, these cells could not fully differentiate into multiciliated ependyma (Figure 4A and 4B; Table S9). Higher percentages of ciliated cells were detected when transplanting EpPs compared with NSCs (Figure 4A and 4B; Table S9).

Pretreatment with MSCs did not increase the percentages of Foxj1+ cells developing cilia from the EpPs (Figure 4A and 4B; Table S9). Surprisingly, the MSC environment decreased the rate of Foxj1+ ciliated cells derived from NSCs (Figure 4A; Table S9).

Effect of Treatment With MSCs on Cilia Development From Cells Committed to the Ependyma Under PHH Conditions

The effect of hemorrhage on ependymal differentiation using primary EpP cell cultures was first studied (Figure 4C and 4D; Table S10). The effect of blood, blood serum, or the inflammatory cytokine TNFα was analyzed, and it was found that they prevent the development of multicilia in Foxj1+ cells (Figure 4C and 4D; Table S10). Interestingly, when Foxj1+ cells were cocultured with MSCs under control conditions (noninflammatory environment), the development of multicilia was hastened (Figure 4C). However, this MSC modulation did not affect the final percentage of differentiated multiciliated ependymal cells (Figure 4C and 4D; Table S10).

The effect of MSCs on the ciliogenesis from EpPs after exposure to TNFα, blood or blood serum was also studied. Interestingly, MSC coculture improved the percentages of Foxj1+ cells developing cilia in the presence of blood serum or TNFα but not whole blood (Figure 4E and 4F; Figure S9; Table S11).

Effects of Stem Cell Therapy on the Brain Parenchyma

The therapeutical impact of the stem cell therapy on damaged brain parenchyma was then studied using our ex vivo ventricular wall explants system after collagenase injection. EpP transplantation into collagenase-induced moderate GMH was selected based on the results of previous experiments (Figures 3C, 3E, and 4A).

The intensity of the Evans blue staining/edema was classified to evaluate the possible effect of the treatment (Figure 5A; Table S12). Transplantation of MSCs revealed a surface reduction of severe edema and increased the area less affected. This effect was apparently higher when both MSCs and EpPs were transplanted (Figure 5A and 5B; Table S12).

Effects of Stem Cell Therapy on the Cytokines Present in the Explant Media

Fold changes were registered in the expression of the cytokines between the MSC-pretreated explants and MSC+EpP-treated explants versus the nontreated explants (Figure 5C; Table S13). The levels of anti-inflammatory cytokines were generally increased in the

Figure 4 Continued. developing cilia at different times in primary cultures and conditions. A control condition is also shown. Mean±SD (bars), n=5 in each condition. *P<0.05, **P<0.01,***P<0.001, ****P<0.0001, ANOVA/Tukey. **D**, Sample pictures used for quantification after 9 d in **C**. Detailed images of 1, 2, and 3 framed areas. **E**, Percentages of EpPs developing cilia. Mean±SEM (bars), n=7 in each condition. **P<0.01,***P<0.001, ****P<0.0001, ANOVA/Tukey. **F**, Sample pictures of cilia development in primary culture of EpPs after 9 d. Details of 1, 2, and 3 framed areas are shown on the **bottom right**. Scale bars: 15 µm (**B**), 30 µm (**D**), and 15 µm (**F**). DAPI indicates 4′,6-diamidino-2-phenylindole; and TNFα, tumor necrosis factor alpha.

Downloaded from http://ahajournals.org by on February 4, 2025

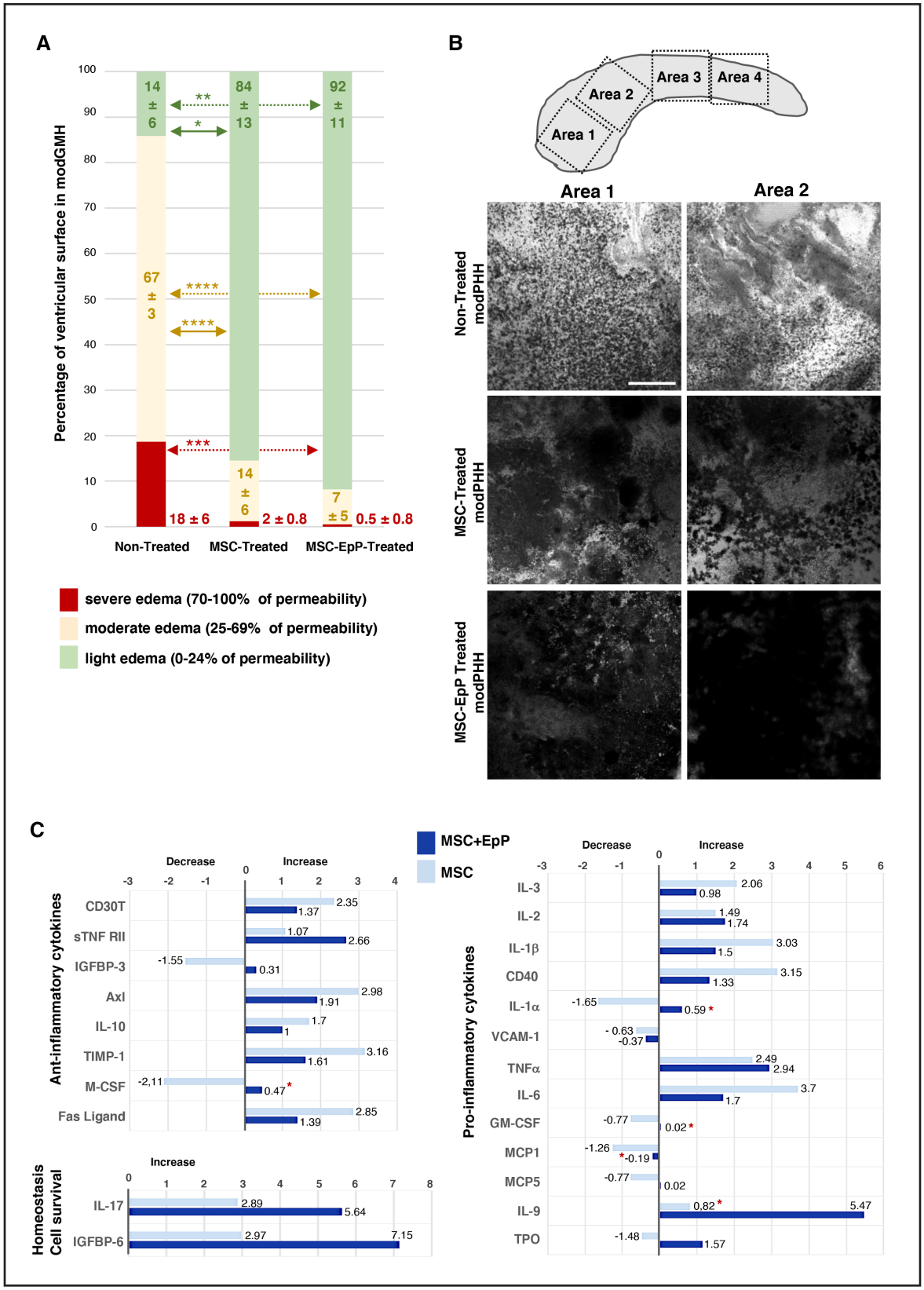

Figure 5. Effect on brain parenchyma after transplantation with ependymal progenitors (EpPs) and mesenchymal stem cells (MSCs). **A**, Percentages of ventricle extensions displaying different degrees of damage stained with Evans blue. Mean±SD, n=6, **P*<0.05, ***P*<0.01, ****P*<0.001, *****P*<0.0001, Kruskal-Wallis/Dunn. **B**, Representative ventricle surface images of **A** corresponding to framed areas 1 and 2 of the explant (drawn on the upper part). **C**, Fold changes compared with the control condition in cytokine content. Positive/negative values indicate increase/decrease vs nontreated explants. Asterisks show nonsignificant differences. Scale bar, 250 µm (**B**). modGMH indicates moderate germinal matrix hemorrhage; and modPHH, moderate posthemorrhagic hydrocephalus.

Downloaded from http://ahajournals.org by on February 4, 2025

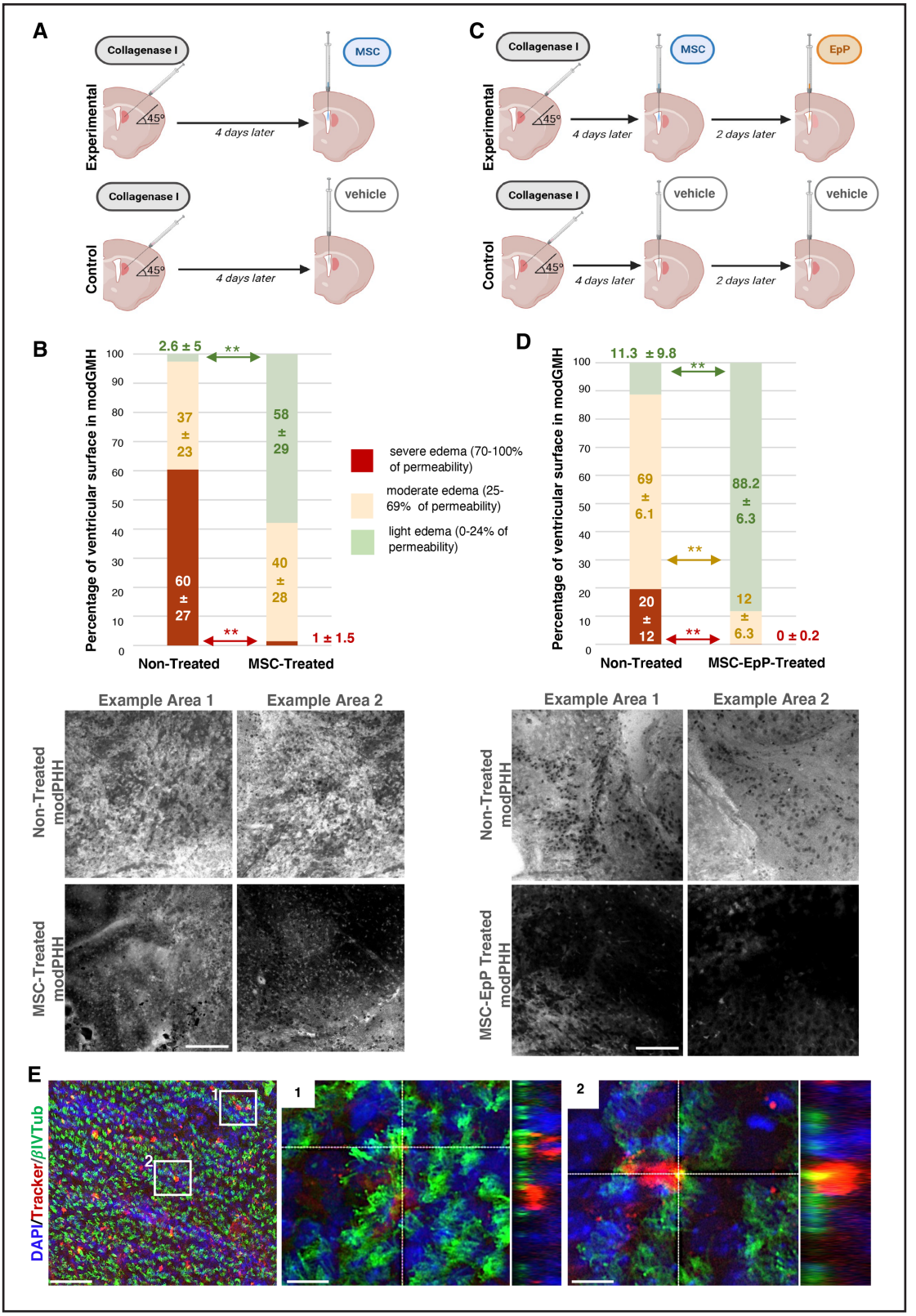

Figure 6. Effect of transplantation with ependymal progenitors (EpPs) and mesenchymal stem cells (MSCs) in vivo. **A** and **C**, Experimental design for MSC treatment (**A**) and MSC-EpP treatment (**B**). **C** and **D**, Percentages of ventricle extensions with Evans blue displaying different degrees of damage after MSC treatment (**C**) and MSC-EpP treatment (**D**). Mean±SD, n=6, $^{**}P<0.01$, Wilcoxon-Mann-Whitney *U* test. Representative images for quantification (**bottom**). Scale bars, 250 µm. **E**, Integration of new multiciliated ependyma derived from transplanted EpPs in the ventricular surface after MSC-EpP treatment. EpP cells are labeled with a cell tracker (red), cilia with βIVTub (βIV-tubulin; green), and nuclei with DAPI (4′,6-diamidino-2-phenylindole; blue). Panoramic view of the ventricle on the **left**. Details of the framed areas 1 and 2 are shown with their pseudo 3-dimensional reconstructions on the **right**. Scale bars, 10 µm. modPHH indicates moderate posthemorrhagic hydrocephalus.

Downloaded from http://ahajournals.org by on February 4, 2025

MSC pretreatment (Figure 5C; Table S13). Cytokines related to cell survival and homeostasis also increased in the MSC pretreatment (Figure 5C).

The results were more variable in the analysis of proinflammatory cytokines (Figure 5C; Table S13).

Combinatory Stem Cell Therapy Induces Recovery of the Ventricular Wall In Vivo

The selected stem cell therapy was then tested in vivo. IVH/GMH was induced by collagenase injection. Results showed a reduction in the severity of the edema after treatment with MSCs and combining both MSCs and EpPs (Figure 6A through 6D; Table S14). Severe edematous areas disappeared, and moderate edema was reduced (Figure 6D) and substituted by light edema, indicating improvement with respect to the control and treatment with only MSCs (Figure 6B). Transplanted EpPs integrated and became multiciliated, indicating that our combined stem cell therapy also induced ependyma restoration (Figure 6E).

DISCUSSION

The present investigation has proved that ependymal disruption and neuroinflammation correlate with the severity of hydrocephalus; repair of the ependyma from NSCs and EpPs is possible in GMH/PHH pathology; and MSC pretreatment improves the therapy.

In premature children with GMH/PHH, NSCs have been obtained from cerebrospinal fluid collected during neuroendoscopic lavage[21] and could, therefore, be used for regenerative purposes.[21] Interestingly, neuroendoscopic lavage can remove blood-derived components, attenuate inflammatory conditions, and thus favor ependymal differentiation. However, our experimental approach shows that EpPs would be more successful in restoring ependyma.

We have found that EpPs can generate ependyma better than NSCs under inflammatory conditions present in GMH/PHH. This difference became more evident after pretreatment with MSCs. In normal conditions, the starting potential of NSCs and EpPs differs and could be key for understanding the present results and their therapeutic implications. Although NSCs display the potential for neuron, oligodendrocyte, and ependymal differentiation in vitro, it has been reported that most NSCs differentiate into astrocytes when transplanted in vivo under inflammatory conditions.[22] Although the transplanted EpPs will be most committed to differentiating into ependymal cells, proinflammatory cytokines can induce the loss of mature ependymal status.[23,24] Both NSCs and EpPs produced more Foxj1+ cells after MSC pretreatment, thus indicating that MSCs generate a more favorable environment to give rise to the cell types preprogrammed to produce.

In the present work, cells derived from EpPs expressing Foxj1 showed alterations in ciliogenesis in the presence of an inflammatory environment, blood components, and TNFα. Normal ependymal differentiation requires the Foxj1 transcription factor,[6,25] and a differentiated multiciliated ependymal state requires constant maintenance of Foxj1.[26] When Foxj1 degradation occurs, multicilia are not maintained, and ependymal cells dedifferentiate. Pretreatment with MSCs on the ependyma could reduce the negative effect of TNFα on ciliogenesis. Previous reports have shown that MSCs, under exposure to high TNFα levels, activate the anti-inflammatory pathway mediated by its receptor TNFR2 (tumor necrosis factor receptor 2)[27] and induce their secretion of anti-inflammatory molecules such as TGFβ (transforming growth factor beta) and IL-10 (interleukin 10).[28]

The tested stem cell therapy also worked in vivo, probably by the sequential nature of the strategy proposed in this work, in which different stem cells are applied and combined for their synergistic effect. These results make this treatment a starting point for future clinical therapies in GMH/PHH in humans.

ARTICLE INFORMATION

Received May 25, 2023; final revision received January 12, 2024; accepted January 24, 2024.

Affiliations

Departamento de Fisiología Humana, Histología Humana, Anatomía Patológica y Educación Física y Deportiva (L.M.R.-P.), Departamento de Biología Celular, Genética y Fisiología (B.O.-P., J.L.-d.-S.-S., M.G.-G.), Departamento de Radiología y Medicina Física, Oftalmología y Otorrinolaringología (D.D.-P.), and Servicios Centrales de Apoyo a la Investigación (C.C.-G.), University of Malaga, Spain. Instituto de Investigación Biomédica de Málaga, Spain (B.O.-P., M.L.G.-M., D.D.-P., A.J.J., P.P.-G.). Department of Neurosurgery, Washington University in St. Louis School of Medicine, MO (M.G.-B.). Unidad de Producción y Reprogramación Celular, Red Andaluza para el diseño y traslación de Terapias Avanzadas, Sevilla, Spain (B.F.-M.). Ikerbasque, Basque Foundation for Science, Bilbao, Spain (R.S.-P.). Instituto de Investigación Sanitaria Biobizkai, Barakaldo, Spain (R.S.-P.). Instituto de Investigación Biomédica de Málaga y Plataforma en Nanomedicina, Spain (M.L.G.-M.).

Acknowledgments

The authors thank David Navas, Jessica Román, and Remedios Crespillo (University of Malaga) for their valuable technical support. Magnetic resonance imaging studies were performed at Infraestructuras Científicas y Técnicas Singulares (ICTS) NANBIOSIS, Unit 28 at Instituto de Investigación Biomédica de Málaga y Plataforma en Nanomedicina.

Sources of Funding

The present work was supported by grants PI19/00778 (Drs Jiménez and Páez-González) and DTS20/00108 (Dr Fernández-Muñoz), Instituto de Salud Carlos III, Spain, cofinanced by the European Union; FPU13/02906 (Dr García-Bonilla), Ministerio de Educación, Cultura y Deporte, Spain; RYC-2014-16980 (Dr Páez-González); Fundación Alicia Koplowitz (Dr Fernández-Muñoz); Ministerio de Economía y Competitividad, Spain; UMA18-FEDERJA-277, Plan Operativo Fondo Europeo de Desarrollo Regional (FEDER) Andalucía 2014-2020 and Universidad de Málaga (Dr Páez-González); Contrato Postdoctoral-Plan Propio de Investigación, Transferencia y Divulgación Científica-Universidad de Málaga (PPITD-UMA), Universidad de Málaga (Dr Rodríguez-Pérez); and Proyectos dirigidos por jóvenes investigadores from Universidad de Málaga (Páez-González).

Disclosures

Dr Sánchez-Pernaute is consultant researcher for Bayer and Novartis. Dr Fernández-Muñoz has research grants from Instituto de Salud Carlos III and Fundación Alicia Koplowitz. The other authors report no conflicts.

Downloaded from http://ahajournals.org by on February 4, 2025

Supplemental Material

ARRIVE Guidelines
Supplemental Methods
Tables S1–S14
Figures S1–S9

REFERENCES

1. Robinson S. Neonatal posthemorrhagic hydrocephalus from prematurity: pathophysiology and current treatment concepts. *J Neurosurg Pediatr*. 2012;9:242–258. doi: 10.3171/2011.12.PEDS11136
2. Strahle J, Garton HJL, Maher CO, Muraszko KM, Keep RF, Xi G. Mechanisms of hydrocephalus after neonatal and adult intraventricular hemorrhage. *Transl Stroke Res*. 2012;3:25–38. doi: 10.1007/s12975-012-0182-9
3. Holste KG, Xia F, Ye F, Keep RF, Xi G. Mechanisms of neuroinflammation in hydrocephalus after intraventricular hemorrhage: a review. *Fluids Barriers CNS*. 2022;19:28. doi: 10.1186/s12987-022-00324-0
4. McAllister JP, Guerra MM, Ruiz LC, Jimenez AJ, Dominguez-Pinos D, Sival D, den Dunnen W, Morales DM, Schmidt RE, Rodriguez EM, et al. Ventricular zone disruption in human neonates with intraventricular hemorrhage. *J Neuropathol Exp Neurol*. 2017;76:358–375. doi: 10.1093/jnen/nlx017
5. Castaneyra-Ruiz L, McAllister JP, Morales DM, Brody SL, Isaacs AM, Limbrick DD. Preterm intraventricular hemorrhage in vitro: modeling the cytopathology of the ventricular zone. *Fluids Barriers CNS*. 2020;17:46. doi: 10.1186/s12987-020-00210-7
6. Jiménez AJ, Domínguez-Pinos MD, Guerra MM, Fernández-Llebrez P, Pérez-Fígares JM. Structure and function of the ependymal barrier and diseases associated with ependyma disruption. *Tissue Barriers*. 2014;2:e28426. doi: 10.4161/tisb.28426
7. Del Bigio MR. Ependymal cells: biology and pathology. *Acta Neuropathol*. 2009;119:55–73. doi: 10.1007/s00401-009-0624-y
8. Bramall AN, Anton ES, Kahle KT, Fecci PE. Navigating the ventricles: novel insights into the pathogenesis of hydrocephalus. *EBioMedicine*. 2022;78:103931. doi: 10.1016/j.ebiom.2022.103931
9. Tan X, Chen J, Keep RF, Xi G, Hua Y. Prx2 (peroxiredoxin 2) as a cause of hydrocephalus after intraventricular hemorrhage. *Stroke*. 2020;51:1578–1586. doi: 10.1161/STROKEAHA.119.028672
10. Lummis NC, Sánchez-Pavón P, Kennedy G, Frantz AJ, Kihara Y, Blaho VA, Chun J. LPA \textsubscript1/3 overactivation induces neonatal posthemorrhagic hydrocephalus through ependymal loss and ciliary dysfunction. *Sci Adv*. 2019;5:eaax2011. doi: 10.1126/sciadv.aax2011
11. Rodríguez EM, Guerra MM, Ortega E. Physiopathology of foetal onset hydrocephalus. In: Limbrick DD, Leonard JR, eds. *Cerebrospinal Fluid Disorders*. Springer International Publishing; 2019:3–30.
12. Henzi R, Vío K, Jara C, Johanson CE, McAllister JP, Rodríguez EM, Guerra M. Neural stem cell therapy of foetal onset hydrocephalus using the HTx rat as experimental model. *Cell Tissue Res*. 2020;381:141–161. doi: 10.1007/s00441-020-03182-0
13. Guerra M. Neural stem cells: are they the hope of a better life for patients with fetal-onset hydrocephalus? *Fluids Barriers CNS*. 2014;11:7. doi: 10.1186/2045-8118-11-7
14. Ahn SY, Chang YS, Sung DK, Sung SI, Yoo HS, Lee JH, Oh WI, Park WS. Mesenchymal stem cells prevent hydrocephalus after severe intraventricular hemorrhage. *Stroke*. 2013;44:497–504. doi: 10.1161/STROKEAHA.112.679092
15. García-Bonilla M, Ojeda-Pérez B, García-Martín ML, Muñoz-Hernández MC, Vitorica J, Jiménez S, Cifuentes M, Santos-Ruíz L, Shumilov K, Claros S, et al. Neocortical tissue recovery in severe congenital obstructive hydrocephalus after intraventricular administration of bone marrow-derived mesenchymal stem cells. *Stem Cell Res Ther*. 2020;11:121. doi: 10.1186/s13287-020-01626-6
16. Vinukonda G, Liao Y, Hu F, Ivanova L, Purohit D, Finkel DA, Giri P, Bapatla L, Shah S, Zia MT, et al. Human cord blood-derived unrestricted somatic stem cell infusion improves neurobehavioral outcome in a rabbit model of intraventricular hemorrhage. *Stem Cells Transl Med*. 2019;8:1157–1169. doi: 10.1002/sctm.19-0082
17. Xie J, Wang B, Wang L, Dong F, Bai G, Liu Y. Intracerebral and intravenous transplantation represents a favorable approach for application of human umbilical cord mesenchymal stromal cells in intracerebral hemorrhage rats. *Med Sci Monit*. 2016;22:3552–3561. doi: 10.12659/msm.900512
18. Ross EJ, Graham DL, Money KM, Stanwood GD. Developmental consequences of fetal exposure to drugs: what we know and what we still must learn. *Neuropsychopharmacology*. 2015;40:61–87. doi: 10.1038/npp.2014.147
19. Lekic T, Manaenko A, Rolland W, Krafft PR, Peters R, Hartman RE, Altay O, Tang J, Zhang JH. Rodent neonatal germinal matrix hemorrhage mimics the human brain injury, neurological consequences, and post-hemorrhagic hydrocephalus. *Exp Neurol*. 2012;236:69–78. doi: 10.1016/j.expneurol.2012.04.003
20. García-Bonilla M, Ojeda-Pérez B, Shumilov K, Rodríguez-Pérez L-M, Domínguez-Pinos D, Vitorica J, Jiménez S, Ramírez-Lorca R, Echevarría M, Cárdenas-García C, et al. Generation of periventricular reactive astrocytes overexpressing aquaporin 4 is stimulated by mesenchymal stem cell therapy. *Int J Mol Sci* . 2023;24:5640. doi: 10.3390/ijms24065640
21. Fernández-Muñoz B, Rosell-Valle C, Ferrari D, Alba-Amador J, Montiel MA, Campos-Cuerva R, Lopez-Navas L, Muñoz-Escalona M, Martín-López M, Profico DC, et al. Retrieval of germinal zone neural stem cells from the cerebrospinal fluid of premature infants with intraventricular hemorrhage. *Stem Cells Transl Med*. 2020;9:1085–1101. doi: 10.1002/sctm.19-0323
22. Mathieu P, Battista D, Depino A, Roca V, Graciarena M, Pitossi F. The more you have, the less you get: the functional role of inflammation on neuronal differentiation of endogenous and transplanted neural stem cells in the adult brain. *J Neurochem*. 2010;112:1368–1385. doi: 10.1111/j.1471-4159.2009.06548.x
23. Gampe K, Brill MS, Momma S, Götz M, Zimmermann H. EGF induces CREB and ERK activation at the wall of the mouse lateral ventricles. *Brain Res*. 2011;1376:31–41. doi: 10.1016/j.brainres.2010.11.040
24. Aubin RG, Troisi EC, Montelongo J, Alghalith AN, Nasrallah MP, Santi M, Camara PG. Pro-inflammatory cytokines mediate the epithelial-to-mesenchymal-like transition of pediatric posterior fossa ependymoma. *Nat Commun*. 2022;13:3936. doi: 10.1038/s41467-022-31683-9
25. Paez-Gonzalez P, Abdi K, Luciano D, Liu Y, Soriano-Navarro M, Rawlins E, Bennett V, Garcia-Verdugo JM, Kuo CT. Ank3-dependent SVZ niche assembly is required for the continued production of new neurons. *Neuron*. 2011;71:61–75. doi: 10.1016/j.neuron.2011.05.029
26. Abdi K, Lai CH, Paez-Gonzalez P, Lay M, Pyun J, Kuo CT. Uncovering inherent cellular plasticity of multiciliated ependyma leading to ventricular wall transformation and hydrocephalus. *Nat Commun*. 2018;9:1655. doi: 10.1038/s41467-018-03812-w
27. Beldi G, Khosravi M, Abdelgawad ME, Salomon BL, Uzan G, Haouas H, Naserian S. TNFα/TNFR2 signaling pathway: an active immune checkpoint for mesenchymal stem cell immunoregulatory function. *Stem Cell Res Ther*. 2020;11:281. doi: 10.1186/s13287-020-01740-5
28. Beldi G, Bahiraii S, Lezin C, Nouri Barkestani M, Abdelgawad ME, Uzan G, Naserian S. TNFR2 is a crucial hub controlling mesenchymal stem cell biological and functional properties. *Front Cell Dev Biol*. 2020;8:596831. doi: 10.3389/fcell.2020.596831

Downloaded from http://ahajournals.org by on February 4, 2025